A functional type II-A CRISPR–Cas system from *Listeria* enables efficient genome editing of large non-integrating bacteriophage

Mario Hupfeld, Despoina Trasanidou, Livia Ramazzini, Jochen Klumpp, Martin J. Loessner and Samuel Kilcher[*]

Institute of Food, Nutrition, and Health, ETH Zurich, Schmelzbergstrasse 7, 8092 Zurich, Switzerland

ABSTRACT

CRISPR–Cas systems provide bacteria with adaptive immunity against invading DNA elements including bacteriophages and plasmids. While CRISPR technology has revolutionized eukaryotic genome engineering, its application to prokaryotes and their viruses remains less well established. Here we report the first functional CRISPR–Cas system from the genus *Listeria* and demonstrate its native role in phage defense. LivCRISPR-1 is a type II-A system from the genome of *L. ivanovii* subspecies *londoniensis* that uses a small, 1078 amino acid Cas9 variant and a unique NNACAC protospacer adjacent motif. We transferred LivCRISPR-1 *cas9* and trans-activating crRNA into *Listeria monocytogenes*. Along with crRNA encoding plasmids, this programmable interference system enables efficient cleavage of bacterial DNA and incoming phage genomes. We used LivCRISPR-1 to develop an effective engineering platform for large, non-integrating *Listeria* phages based on allelic replacement and CRISPR-Cas-mediated counterselection. The broad host-range *Listeria* phage A511 was engineered to encode and express lysostaphin, a cell wall hydrolase that specifically targets *Staphylococcus* peptidoglycan. In bacterial co-culture, the armed phages not only killed *Listeria* hosts but also lysed *Staphylococcus* cells by enzymatic collateral damage. Simultaneous killing of unrelated bacteria by a single phage demonstrates the potential of CRISPR–Cas-assisted phage engineering, beyond single pathogen control.

INTRODUCTION

CRISPR–Cas loci encode adaptive defense systems designed to protect bacteria from bacteriophage (phage) infection and other invading DNA elements. These systems comprise a protein machinery that incorporates short sequences of incoming phage DNA (known as protospacers) into a bacterial sequence repeat array locus called CRISPR [1,2]. Once integrated into the CRISPR array, the phage-derived sequences are referred to as spacers. Pre-CRISPR RNA (pre-crRNA) is transcribed from the array and processed to yield short, phage-derived RNA-templates (crRNA) to be integrated into a nuclease-targeting complex. This RNA-guided interference complex recognizes and cuts corresponding phage DNA in a sequence-specific fashion, thereby conveying immunity to the bacterium [2–5]. To date, six CRISPR–Cas types have been described, which feature highly diverse *cas* gene content and operon organization. To prevent targeting of the CRISPR array, many systems require a protospacer adjacent sequence motif (PAM) for interference, which is found in the targeted DNA, but absent from the genomic CRISPR locus. With only three to four *cas* genes (*cas9*, *cas1*, *cas2* and *cas4* or *csn2*), type II systems belong to the simplest CRISPR-Cas loci known. They are defined by characteristic operon organization, presence of the *cas9* nuclease gene, and a small trans-activating crRNA (tracrRNA). For interference, type II systems require *cas9*, tracrRNA, crRNA and host RNAseIII, while *cas1*, *cas2* and *cas4*/*csn2* are dispensable [5,6]. Type II systems have been adapted for man applications, especially for the targeted modification of eukaryotic genomes [7,8]. Based on the rapid development of the technology, CRISPR–Cas is now being used in eukaryotic and prokaryotic systems and is expanding to functions beyond DNA-cleavage, including targeted transcriptional regulation and DNA modification [9–12]. Even though phages are natural CRISPR targets, only few CRISPR–Cas systems for targeted modification of phage genomes have been reported [13–19]. This is surprising, especially considering that genome engineering of strictly lytic, non-integrating phages is a difficult and labor-intensive process (reviewed by Pires *et al.* [20]).

---

[*]To whom correspondence should be addressed. Tel: +41 44 633 89 33; Email: samuel.kilcher@hest.ethz.ch

Bioinformatics reveal putative CRISPR–Cas systems in approximately 10% of bacterial genomes (21) (or in 40–50% of cultivatable bacteria (22,23)), yet experimental proof of *in vivo* activity is scarce. With respect to the intracellular pathogen *Listeria monocytogenes*, a comparative analysis of 128 strains showed that 41.4% contain putative *cas* genes, and a recent study by Rauch *et al*. demonstrated weak activity of a *Listeria* type II CRISPR–Cas system against plasmids carrying cognate spacer and PAM sequences (24,25). However, activity of native *Listeria* CRISPR–Cas systems against naturally occurring phage has not been demonstrated, possibly because *L. monocytogenes* strains frequently contain prophage-encoded anti-CRISPR proteins (25). CRISPR–Cas systems have also been identified in the animal pathogen *L. ivanovii* but their functionality has not been tested (26,27).

In this study, we report the characterization of two CRISPR loci (LivCRISPR-1 and LivCRISPR-2) identified in the genome of *L. ivanovii* subspecies (ssp.) *londoniensis* WSLC 30167 and provide evidence that LivCRISPR-1 contributes to phage resistance in this strain. In addition, we constructed a LivCRISPR-1-based, programmable, sequence-specific nuclease system that is transferable to other species of the genus *Listeria*. The small LivCRISPR-1 Cas9 protein allows for efficient, targeted cleavage of *Listeria* and phage DNA and enables editing of virulent *Listeria* phage genomes. Using LivCRISPR-1, we produced a genetically armed *Listeria* phage that induces the production and release of a *Staphylococcus*-specific cell wall hydrolase from infected cells, and thus allows for control of both bacteria in co-culture. In the future, this approach should be useful for the control and modification of complex bacterial environments, including the possibility to balance and shape specific microbiomes.

MATERIALS AND METHODS

Bacterial strains, bacteriophages, plasmids, and primer

L. monocytogenes and *L. ivanovii* strains were cultivated in 1/2 BHI medium at 30°C. *E. coli* XL1-blue and *S. aureus* ATCC19685 were cultivated in LB medium at 37°C. Phages B025, B035, B056, P40, and A511 were propagated on *L. ivanovii* WSLC 3009 at 30°C, B054 was propagated on WSLC 3009 at 19°C, and P35 was propagated on *L. monocytogenes* Mack at 20°C. Phage infection assays were carried out using the soft agar overlay method. Briefly, 10 μl phage dilution was mixed with 200 μl stationary host culture in 4 ml LC soft agar (10 g/l tryptone, 5 g/l yeast extract, 10 g/l glucose, 7.5 g/l NaCl, 10 mM $CaCl_2$, 10 mM $MgSO_4$, 0.4% agar) at 46°C and poured onto agar plates (1/2 BHI plates for B025, B035, B054, B056, P40 and A511; LC plates for P35). Plaque-forming units (pfus) were quantified at six (B054) or one (all other phages) days post infection. All plasmids and primers can be found in Supplementary Tables S1 and S2.

Phage adsorption assays

To quantify phage adsorption, 490 μl of SM-Buffer containing 0.02% Tween20 and 2 mM $CaCl_2$ were mixed with 10^9 *Listeria* cells. 10 μl of phage dilution containing 10^7

phages and 500 μl 1/2 BHI medium were added. Tubes without *Listeria* cells served as phage input control. Samples were incubated for 10 min on an overhead rotator at 20°C and centrifuged for 2 min (12 000 × g, 4°C). Supernatants were transferred to new reaction tubes and pellets suspended in 1 ml SM buffer on ice. Serial dilutions of both fractions were prepared and pfus quantified.

Cell wall decoration with fluorescent affinity proteins

Cell wall-binding domains (CBDs) derived from the endolysins of *Listeria* phage A500 and *S. aureus* phage 2638A have previously been engineered as GFP (GFP-CBD500) or dsRed (dsRed-CBD2638A) fusion proteins that allow for selective staining of their respective host (see (28)): 0.5 ml bacterial culture (OD = 1) was harvested (1 min, 7500 g, 4°C), resuspended in 100 μl SM-buffer containing 10 μg of dsRed-CBD or GFP-CBD protein, incubated for 2 min at RT on an overhead rotator, washed twice with 1 ml cold SM-buffer, and finally suspended in 50 μl SM-buffer. 4 μl of stained cultures were spotted onto a microscopy slide and visualized on a Leica TCS SPE confocal system (Leica Microsystems, Germany) equipped with a HCX PL FLUO-TAR 100.0 × 1.30 oil objective.

Bioinformatics

Homology searches were performed using BLAST (29), weblogo was used for visualization of the PAM (30), and *cas* gene homologies were identified using HHPred (31). To identify putative tracrRNA sequences, CRISPR repeats were aligned with the complete *cas*-gene region using BLASTn. Identified regions of homology were analyzed for the presence of a bacterial promoter (using BPROM, a sigma70 promoter prediction software) and terminator (using the ARNold software, http://rna.igmors.u-psud.fr/toolbox/arnold) in the 5′ and 3′ regions, respectively (32–35). Multiple alignments of Cas9 proteins were performed using CLC Workbench (version 9.5.4; Qiagen; settings: progressive alignment, gap open cost = 10, gap extension cost = 1, end gap cost = as any other). Information on the proteins used to create the alignment can be found in Supplementary Table S4. Phylogenetic trees were constructed using CLC Workbench (tree construction method = neighbor joining, protein distance measure = Jukes-Cantor, bootstrap analysis = 100 replicates).

Transformation of *Listeria*

Listeria electrocompetent cells were prepared according to a modified protocol by Monk *et al*. (36). 40 ml 1/2 BHI + 0.5 M sucrose were inoculated with 2 ml stationary phase culture and incubated at 30°C (shaker, 180 rpm) until an OD_{600nm} of 0.2 was reached. Each liquid culture was distributed into four 10 ml aliquots and cells were grown for 2 h at 30°C in the presence of different concentrations of penicillin G (5, 10, 25, 50 μg/ml). For transformation of WSLC 3009, WSLC 1042, and Mack, 10 μg/ml lysozyme was added during the last 10 minutes of incubation. Cells were chilled on ice for 5 min, transferred to a 50 ml Falcon tube, and pelleted by centrifugation (4000 × g, 10 min,

4°C). The pellet was washed once with 1.5 ml and once with 1 ml of cold sucrose-glycerol washing buffer (SGWB; 0.5 M sucrose, 10% glycerol, pH 7.4) before final resuspension (60 µl SGWB per transformation). 1.5 µg plasmid DNA were mixed with 60 µl of electrocompetent cells and transferred to a cold 2 mm electroporation cuvette. *Listeria* cells were electroporated (2.2 kV/cm 400 Ohm, 25 µF) using a Gene Pulser™ (BioRad Laboratories) and recovered with 1 ml warm 1/2 BHI + 0.5 M sucrose at 30°C for 90 min. Cultures were plated on 1/2 BHI agar plates supplemented with antibiotics (50 µg/ml kanamycin, 5 µg/ml erythromycin, or 10 µg/ml chloramphenicol).

Gene deletion in *Listeria*

Generation of *cas* gene deletion mutants (ΔCas(LivCR-1), ΔCas(LivCR-2) and ΔΔCas(LivCR-1/2)) was performed using splicing-overlap-extension (SOE) PCR (37,38), followed by allelic exchange mutagenesis. SOE primers were designed to amplify ∼500 bp sequences flanking the *cas* gene regions of interest. Flanking fragments were fused using SOE-PCR with primer P76/P79 for ΔCas(LivCR-1) and P80/P83 for ΔCas(LivCR-2). Editing templates were digested, ligated into the pAULA, and transformed into *E. coli* XL1 blue (39). The editing template to construct the WSLC 30167 ΔBREX mutant was synthesized (Thermofisher Scientific), amplified with primers P100 and P101, and cloned into pAULA. Sequenced editing vectors were transformed into WSLC 30167 by electroporation. Homologous recombination of the plasmid with the genome was selected for by shifting to non-permissive conditions (39°C). After six passages, the antibiotic resistant strains were inoculated into 1/2 BHI without antibiotics at permissive temperatures (30°C). After another five passages, single colonies were screened for loss of erythromycin resistance. Sensitive colonies were screened by PCR for deletion of target genes and PCR products sequenced.

Construction of LivCRISPR-1 pre-crRNA expressing vector pLRSR scr

A DNA fragment containing the endogenous leader sequence of LivCRISPR-1 (220 bp sequence upstream of the first repeat unit of LivCRISPR-1) followed by one repeat-spacer-repeat (RSR) unit and 350 bp of sequence downstream of the last endogenous repeat unit was synthesized. This synthetic CRISPR array was cloned into the *E. coli-Listeria* shuttle vector pLEB579 (40) using restriction enzyme *Xba*I to yield the pre-crRNA vector pLRSR scr. The spacer region of pLRSR scr contains two BsaI sites that enable incorporation of any spacer sequence of choice using annealed oligonucleotides, essentially as described by Jiang et al. (41). Appropriate *Bsa*I overhangs need to be reconstituted to generate functional RSR units upon ligation with *Bsa*I-digested pLRSR scr (see Figure 3A). For annealing, 50 µl oligonucleotide pairs (4 µM each) were mixed in T4 ligase buffer, heated to 100°C for 10 min, and slowly cooled to RT in a heating block. Annealed spacers were ligated with *Bsa*I-digested pLRSR scr, transformed into *E. coli* XL-1 blue cells, and grown on LB plates supplemented with 300 µg/ml erythromycin. All pLRSR-derived plasmids and

oligonucleotide sequences can be found in Supplementary Tables S1 and S2.

Transfer of *cas9* and tracrRNA into *Listeria*

For genomic expression of LivCRISPR-1 *cas9* and tracrRNA from their endogenous promoter, the *cas9* 5′-region (360 bp), *cas9* gene, and tracrRNA were amplified from using primers P1 and P2 and cloned into the integrative plasmid pIMK (42) to yield pIMK P_{end} *cas9*. For overexpression, *cas9* and tracrRNA were amplified without the *cas9* 5′ region using primers P3 and P4 and cloned into pIMK2 to yield pIMK2 P_{help} *cas9*. *Listeria* strains were transformed with both plasmids and integration selected for with 50 µg/ml kanamycin.

CRISPR-Cas-mediated targeting of bacterial and phage genomic DNA

To target bacterial gDNA, *Listeria* cells were electroporated with 1.5 µg of pLRSR plasmid expressing a pre-crRNA that targets the DNA polymerase I gene of the transformed *Listeria* strain (self-targeting vector). As control, 1.5 µg of a non-targeting pre-crRNA plasmid (pLRSR scr) was used. Transformed cells were grown on 1/2 BHI plates supplemented with 5 µg/ml erythromycin for 48 h at 30°C, colony forming units quantified by plating serial dilutions, and relative transformation efficiencies calculated. To target phage genomic DNA, LivCRISPR-1 *cas9* and tracrRNA expressing propagation strains were transformed with pre-crRNA plasmids targeting late genes of phages P40 (pLRSR P40; targets the putative tail tape measure protein gp14), A511 (pLRSR A511; targets the putative tail tip protein gp028), and P35 (pLRSR P35; targets the putative tail tape measure protein gp14). Plasmids were constructed as described in Supplementary Tables S1 and S2. Artificial bacteriophage-insensitive mutants (BIMs) were tested for phage sensitivity using spot-on-the-lawn assays: 200 µl over-night culture was mixed with 4 ml soft-agar and poured on bottom-agar in a 10 cm petri dish. Once solidified, serial phage dilutions (10 µl) were spotted on this plate and incubated over-night.

LivCRISPR-1-assisted site-directed mutagenesis of phage A511

Eight editing plasmids with homology regions flanking both sides of the protospacer and PAM sequence were constructed using shuttle vector pSK1 as a backbone. Four plasmids contained one mutation in the PAM (NNA**C**AC to NNA**T**AC) and 400, 250, 150 or 50 bp homology arms on each side. The remaining four plasmids contained four additional silent mutations (see Figure 5B) and the same homology arms. Flanking regions were amplified by PCR using primers containing the mutated spacer/PAM sequences, purified, and assembled with the pSK1 plasmid backbone using the Gibson Assembly method (NEBuilder HiFi DNA Assembly Cloning Kit) to yield the editing plasmids. A511 gp97 crRNA targeting construct was cloned by incorporation of annealed oligonucleotides P13 and P14 into BsaI-digested pLRSR scr to yield pLRSR A511. Mutant phages were isolated using a one-step protocol: The

WSLC 3009::Phelp *cas9* strain containing pSK1-derived editing plasmids and the A511-targeting pre-crRNA plasmid (pLRSR gp97) was infected with serial dilutions of A511 wild type phages using the soft-agar overlay assay. Two phage plaques were sequenced to validate genotype.

Construction of lysostaphin-encoding A511::*lst* phages

Pre-crRNA expression plasmids targeting the endolysin or major capsid gene of A511 were constructed as described above using primers P62 and P63 (pLRSR A511 ply) or P64 and P65 (pLRSR A511 cps), respectively. The editing plasmids containing flanking homology arms and the lysostaphin-hexahistidine (his6) gene sequence (771 bp + ribosomal binding site: GAGGAGGTAAATATAT) were assembled into the pSK1 backbone as described in Supplementary Tables S1 and S2. Silent mutations were subsequently introduced into the PAM motif of these editing plasmids using site-directed mutagenesis to allow for CRISPR escape of recombinant phage genomes. The final editing plasmids pSK1 ply511 lst-his6 and pSK1 cps511 lst-his6 mediate integration of the lysostaphin-his6 gene downstream of the A511 endolysin (*ply511*) and major capsid gene (*cps511*), respectively. First, *L. ivanovii* WLSC 3009 was transformed with either of the two editing plasmids and infected with A511 wild type phage using the soft-agar overlay technique to obtain semi-confluent lysis. The obtained phage lysate was subsequently titered on WSLC 3009::P$_{help}$_*cas9* pLRSR_A511ply or WSLC 3009::P$_{help}$_*cas9* pLRSR_A511 cps. Four candidate plaques were picked for each phage and assayed for the correct genotype using PCR and sequencing (see Supplementary Figure S6).

Infection of *Listeria* and *Staphylococcus* co-cultures

Stationary phase cultures of WSLC 3009 and/or ATCC19685 were diluted in 1/2 BHI to obtain an OD of 0.1 (OD = 0.05 of each strain for co-culture infections). 15 ml of the cultures were incubated at 30°C for 1 h before phage addition ($t = 0$) at a multiplicity of infection (moi) of 0.03. Infected cultures were incubated (30°C) and optical density monitored for 320 minutes. In addition, serial dilutions were plated on selective Oxford (*Listeria*) and Baird-Parker (*Staphylococcus*) agar plates (biolife) at 0, 100, 200 and 300 min post infection. Cfus were counted after 24 h incubation at 30 or 37°C, respectively.

Purification of lysostaphin-his6 from phage infected cultures

One liter of prewarmed 1/2 BHI medium was inoculated with 20 ml of a WSLC 3009 overnight culture. Phages (A511::*lst1* or A511::*lst2*) were added to a final concentration of 1×10^5 pfu/ml. After 3–4 h at 30°C more phages were added to a final concentration of 1×10^7 pfu/ml and incubated for another 3 h. Cleared lysates were centrifuged (10 000 × g, 10 min) and supernatants incubated with 10 ml Ni-NTA Superflow resin (Qiagen) at 4°C for 30 min on an overhead rotator. Resin was transferred to MicroBiospin columns (Bio-Rad) and washed extensively with buffer A (500 mM NaCl, 50 mM Na$_2$HPO$_4$, 5 mM imidazole, 0.1% Tween 20 [pH 8.0]). His-tagged lysostaphin was eluted using Buffer B (500 mM NaCl, 50 mM Na$_2$HPO$_4$, 250 mM imidazole, 0.1% Tween 20 [pH 8.0]). Pooled fractions were dialyzed twice against dialysis buffer (NaH$_2$PO$_4$, 120 mM NaCl [pH 8.0], 0.01% Tween 20) and samples assayed by SDS-PAGE.

RESULTS

### *Listeria ivanovii* ssp. *londoniensis* are highly resistant to phage infection

Listeria strains are grouped into serovars, based on both H (flagellar) and O (cell surface-associated) antigens (43,44). *L. ivanovii* strains all belong to serovar 5 and thus share similar cell-wall architecture (45). The primary differences between the two *L. ivanovii* subspecies (spp. *londoniensis* and spp. *ivanovii*) are the lack of ribose fermentation and, more interestingly, a high degree of intrinsic phage resistance observed for ssp. *londoniensis* isolates (26,46). Using the API test (Supplementary Figure S1), we identified four ssp. *londoniensis* strains (WSLC 3060, WSLC 30130, WSLC 30151 and WSLC 30167) from our collection. Soft-agar overlay infection assays with *Listeria* phages A511, B025, B035, B054 and B056 (47) were performed to determine the susceptibility of four ssp. *londoniensis* and five ssp. *ivanovii* strains (Figure 1A). While the strictly lytic, broad host-range Myovirus A511 (48) infected all strains, the other temperate Siphoviruses either failed to plaque, or revealed a markedly reduced efficiency of plating (eop) on *Listeria* ssp. *londoniensis*. This led us to hypothesize that ssp. *londoniensis* strains might employ specific defense mechanisms not found in other *L. ivanovii* strains.

Multiple phage resistance mechanisms are active in *L. ivanovii* ssp. *londoniensis*

To escape phage predation, mutations are frequently found in bacterial genes that mediate the glycosylation of wall teichoic acids (WTA), which constitute the binding ligands for most *Listeria* phages (49–51). To test whether host cell binding of B025, B035, B054 and B056 is affected in phage-resistant ssp. *londoniensis* strains, we employed adsorption assays using ssp. *ivanovii* strain WSLC 3009 as positive control (Figure 1B). Surprisingly, only WSLC 3060 and WSLC 30151 showed abrogated phage binding, while phages bound normally to the surface of the other ssp. *londoniensis* strains. This suggests that strains WSLC 30130 and WSLC 30167 possess intracellular mechanisms that interfere with productive phage infection. Therefore, phage resistance of the analyzed ssp. *londoniensis* strains is conveyed by at least two different mechanisms.

Two different type II-A CRISPR–Cas systems in *L. ivanovii* WSLC 30167

To identify intracellular phage resistance mechanisms in ssp. *londoniensis*, we compared the genome sequences of phage-permissive WSLC 3009 and phage-resistant WSLC 30167 strains (26,27). We identified two independent CRISPR–Cas systems in WSLC 30167 (designated LivCRISPR-1 and LivCRISPR-2) that feature distinct
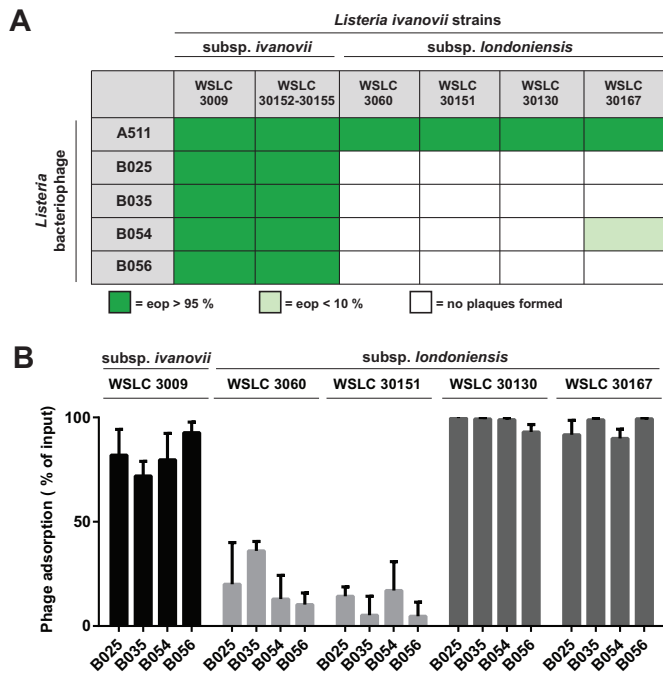
Figure 1. Different mechanisms mediate phage resistance of *L. ivanovii* ssp. *londoniensis*. (**A**) Sensitivity of five *L. ivanovii* ssp. *ivanovii* and four ssp. *londoniensis* strains to broad host-range phage A511 and serovar-specific temperate phages B025, B035, B054, and B056 was determined at the optimal propagation condition of each phage. Plating efficiencies were determined from soft-agar overlay infection assays with serial dilutions of the indicated phages. (**B**) Binding of B025, B035, B054, and B056 to phage-sensitive ssp. *ivanovii* and phage-resistant ssp. *londoniensis* strains was determined using phage adsorption assays. Data are presented as mean ± SD from three biologically independent experiments. Eop = efficiency of plating relative to WSLC 3009; SD = standard deviation.

direct repeat sequences and *cas* genes. In contrast, no CRISPR–Cas system was found in the genome of WSLC 3009. LivCRISPR-1 is large, comprising a 6284 bp CRISPR array (nucleotide positions 534 160–540 443). It contains 95 spacers, 29–32 bp in length, of which seven showed 100% sequence identity to known *Listeria* phage genomes (Figure 2A (red bars); more details in Supplementary Figure S2A and Supplementary Table S4). The CRISPR array of the second CRISPR–Cas system (LivCRISPR-2) is significantly smaller (1056 bp, positions 2 761 818–2 762 873) and encodes only 16 spacers, 30 bp in length, none of which shared full sequence identity with any known phage (Figure 2A, bottom). Upstream of both CRISPR array regions, we identified *cas9, cas1, cas2* and *csn2* genes, as well as tracrRNA elements, classifying them as type II-A systems (Supplementary Figure S2B and C, Supplementary Table S3). We performed a phylogenetic analysis of representative type II-A Cas9 orthologs (52) (Figure 2B, Supplementary Figure S3, and Supplementary Table S4) and found that LivCRISPR-2 Cas9 clusters with other *Listeria* CRISPR systems. In contrast, LivCRISPR-1 Cas9 is not closely related to previously known *Listeria* CRISPR-systems but rather clusters with small Cas9 variants from *Staphylococcus, Eubacterium,* and *Clostridium,* including a previously described, highly active Cas9 protein from *S. aureus* (53,54). To identify a PAM for

LivCRISPR-1, we aligned the protospacer-flanking regions of six known target genomes (see Supplementary Table S5). We found a conserved NNACAC motif immediately downstream of the protospacer sequences (Figure 2C), which has not previously been reported for other CRISPR–Cas systems (30,55,56).

LivCRISPR-1 contributes to native phage resistance in *L. ivanovii* ssp. *londoniensis*

To assess the functionality of LivCRISPR-1 and LivCRISPR-2 as potential phage resistance mechanisms in WSLC 30167, we designed several *cas* gene deletion mutants (39). First, the *cas* gene cassettes (*cas9, cas1, cas2* and *csn2*) of each WSLC 30167 CRISPR–Cas system were deleted individually, resulting in strains ΔCas(LivCR-1) and ΔCas(LivCR-2). Next, a ΔΔCas(LivCR-1/2) double deletion mutant was constructed, which is devoid of all *cas* genes. We challenged the mutants with phage B054, for which a spacer with 100% identity was identified in the LivCRISPR-1 array. Deletion of LivCRISPR-1 *cas* genes led to complete restoration of phage sensitivity, while LivCRISPR-2 was not required for B054 interference (Figure 2D). This finding demonstrates that LivCRISPR-1 is actively involved in B054 resistance *in-vivo*. It was not possible to determine the putative relevance of native LivCRISPR-2 in this assay, because no spacer sequence with identity to any known *Listeria* phage is present and because its PAM could not be determined with certainty. Even though LivCRISPR-1 contains two B025-targeting spacers, all *cas*-gene deletion mutants remained insensitive to this phage, suggesting that additional defense mechanisms are restricting this phage.

Functional LivCRISPR-1 can be transferred to and engineered in *L. monocytogenes*

Our findings demonstrate that LivCRISPR-1 is actively involved in *L. ivanovii* phage defense. To assess whether the system can be engineered as a programmable, sequence-specific nuclease, we designed a LivCRISPR-1-based CRISPR-RNA plasmid encoding a leader-repeat-spacer-repeat unit with exchangeable spacer sequence (pLRSR scr), which allows for the expression of small custom-designed pre-crRNAs (Figure 3A) (17). In a self-targeting assay (25), pLRSR was directed against the DNA-polymerase I gene of the LivCRISPR-1-encoding strain WSLC 30167 (pLRSR 30167 DNA pol.I). The transformation efficiency with this self-targeting pLRSR plasmid dropped to ∼3%, compared to the non-targeting control (pLRSR scr, Figure 3B). The 3% escapers were not due to weak interference activity but instead featured deletions of the repeat-spacer-repeat unit in pLRSR 30167 DNA pol.I (Supplementary Figure S4). Transformation efficiency of the self-targeting plasmid was rescued in ΔCas(LivCR-1) and ΔΔCas(LivCR-1/2) strains, confirming that self-targeting was dependent on *cas* genes of LivCRISPR-1 (Figure 3B). To determine the minimal requirements for CRISPR interference, *cas9* and tracrRNA of LivCRISPR-1 were transferred to the genome of WSLC 30167 ΔCas(LivCR-1) using integrative, pIMK-based plas-
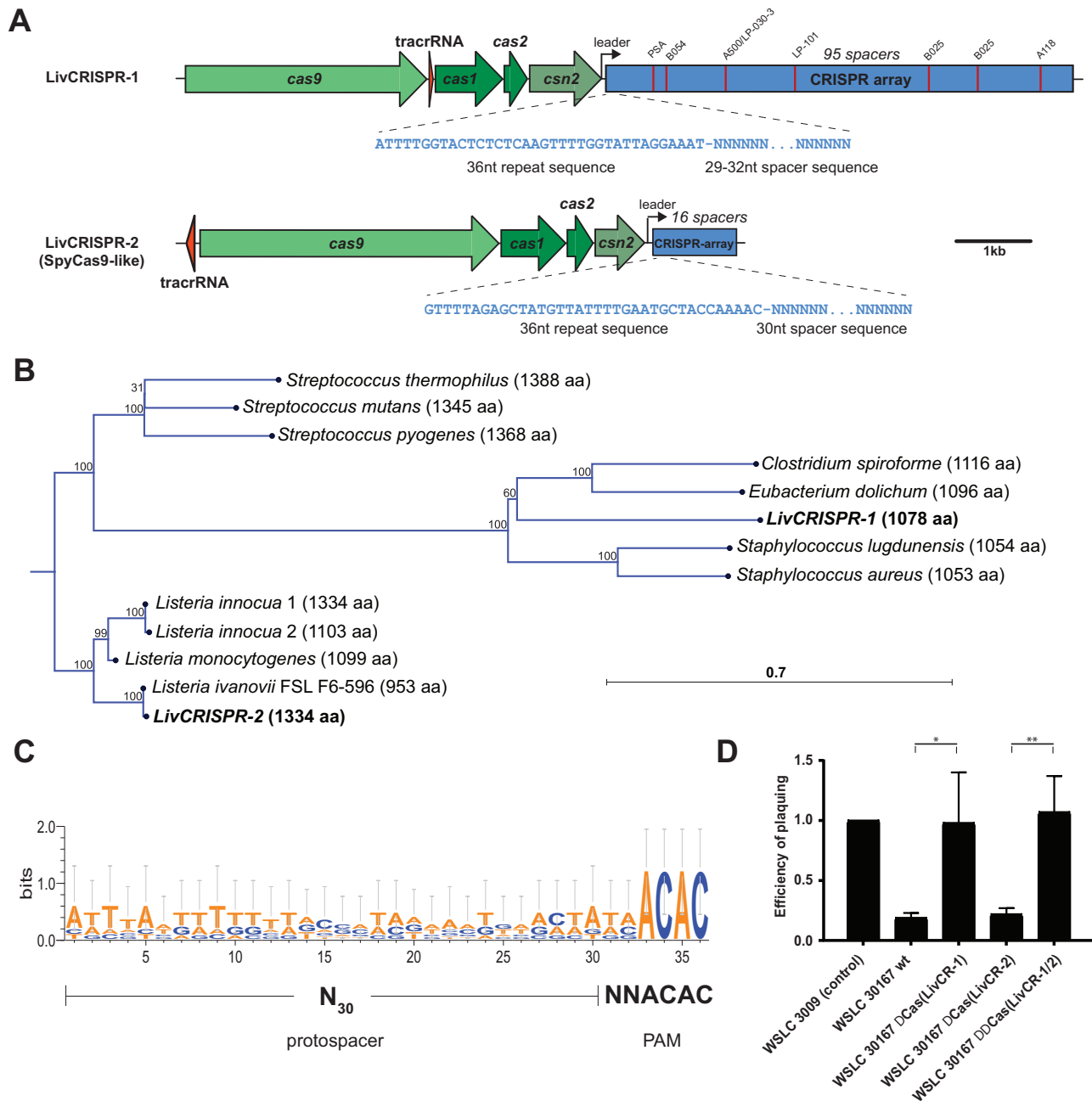
Figure 2. (**A**) Two CRISPR–Cas systems (LivCRISPR-1 and LivCRISPR-2) were identified in the genome of WSLC 30167 using CRISPRfinder as well as HHpred structure predictions of CRISPR array-associated genes (Supplementary Table S3). Schematic representations of the CRISPR loci including *cas* genes, CRISPR array, and tracrRNA are shown. Red bars in the CRISPR array indicate spacers with 100% sequence identity to known *Listeria* phage genomes. (**B**) Phylogenetic tree constructed from multiple sequence alignment of LivCRISPR-1/2 Cas9 proteins and 11 representative Cas9 orthologs. (**C**) LivCRISPR-1 PAM was deduced by aligning extended protospacer regions of six known phage genomes that are targeted by LivCRISPR-1. Spacer 24 was excluded from analysis because it was assigned to two phages with different PAMs. (**D**) Phage B054 sensitivity of WLSC 30167 wild type and *cas*-gene deletion mutants was assessed using infection assays. Eop relative to strain WSLC 3009 is shown. Data are presented as mean ± SD from three biologically independent experiments. Student's *t*-tests were performed ($P < 0.05$ (*), $P < 0.01$ (**)). aa = amino acid. SpyCas9 = canonical *S. pyogenes* Cas9.

mids (42). Cas9 and tracrRNA expression was driven either from the putative, endogenous *cas9* promoter region (P_{end} *cas9*), or from a strong, constitutive promoter (P_{help} *cas9*). Self-targeting assays demonstrated that chromosomal expression of *cas9* and tracrRNA was sufficient to rescue CRISPR-activity in WSLC 30167 ΔCas(LivCR-1), as long as *cas9* was expressed from P_{help} (Figure 3B). This minimalized CRISPR–Cas system was transferred to *L. ivanovii* ssp. *ivanovii* (WSLC 3009) and *L. monocytogenes* (WSLC 1042), again using integrative pIMK-based plasmids. Self-targeting assays directed against their respective DNA polymerase I genes demonstrated that LivCRISPR-1 was fully active in these related species as well (Figure 3C and D). Expression from the endogenous *cas9* promoter region did not
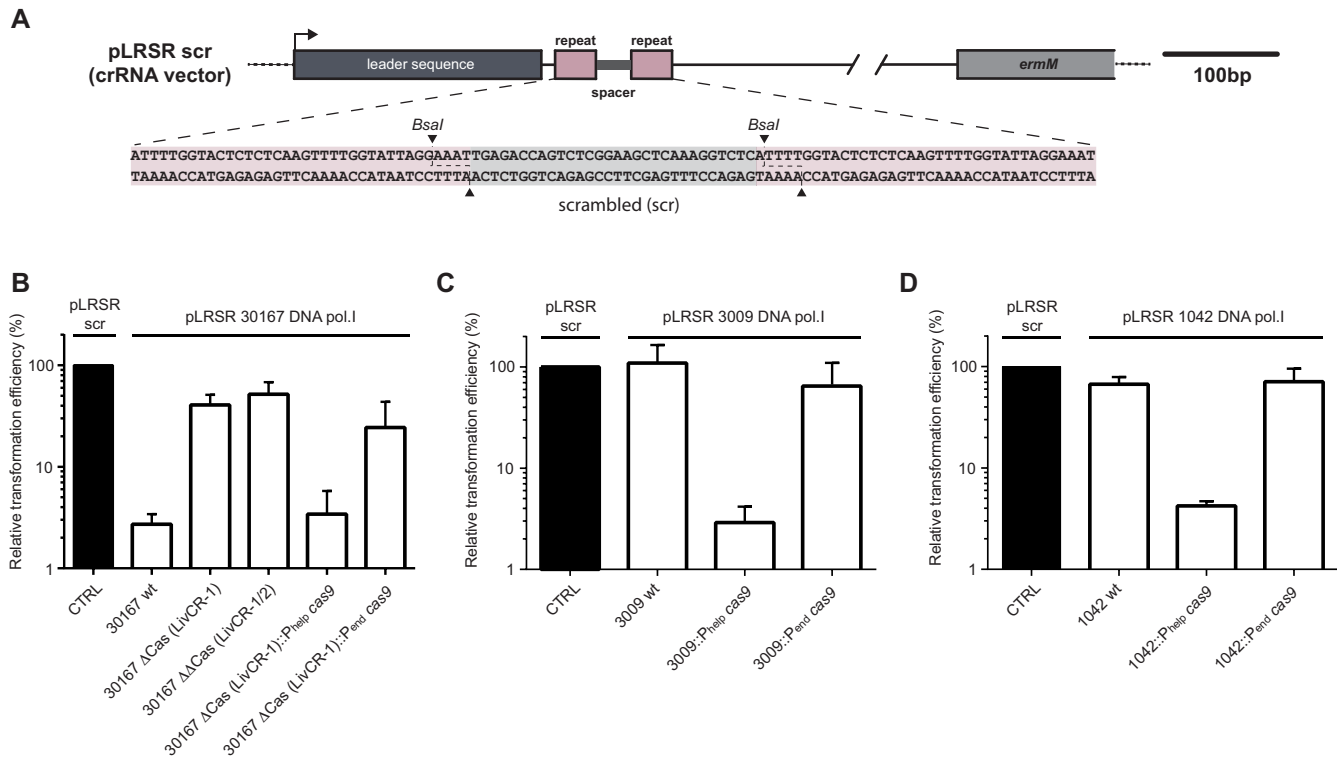
Figure 3. Programmable LivCRISPR-1 Cas9 targets bacterial DNA and is transferrable to *L. monocytogenes*. (**A**) Schematic representation of the pLRSR scr plasmid used as a backbone to express LivCRISPR-1 pre-crRNAs. Spacer sequences are inserted into *Bsa*I-digested pLRSR scr using annealed oligonucleotides with appropriate 3′-overhangs. (**B–D**) Self-targeting assays: To quantify CRISPR activity, transformation efficiencies of DNA polymerase targeting pre-crRNA plasmids were compared with non-targeting controls (pLRSR scr, CTRL). Interference activity of LivCRISPR-1 was assayed in (**B**) WSLC 30167 wild type, LivCRISPR-1/2 deletion mutants, and *cas9*/tracrRNA reconstituted strains. Furthermore, LivCRISPR-1 *cas9* and tracrRNA were transferred to (**C**) *L. ivanovii* ssp. *ivanovii* (WSLC 3009) and (**D**) *L. monocytogenes* (WSLC 1042) strains and tested for activity. Data are presented as mean ± SD from three biologically independent experiments.

result in detectable activity, suggesting that *cas* genes were expressed from a large operon, or are subject to context-dependent regulation in WSLC 30167. Collectively, these experiments demonstrate that *Listeria* genomes can be targeted using pre-crRNA expression plasmids and that heterologous expression of *cas9*, tracrRNA, and pre-crRNA is sufficient for full interference activity in both *L. ivanovii* and *L. monocytogenes*.

Engineered CRISPR–Cas9 can control infection by non-integrating bacteriophages

The engineered CRISPR–Cas9 system was tested for its ability to confer resistance to infection by strictly lytic, non-integrating *Listeria* phages. Three pre-crRNA plasmids (pLRSR-based) were constructed, which contained spacers that target late genes of the virulent Siphoviruses P35 (pLRSR P35) and P40 (pLRSR P40), as well as the Myovirus A511 (pLRSR A511) (see Materials and Methods) (48,57). We generated phage propagation strains that express the required tracrRNA and *cas9* gene from their genomic DNA. These strains were transformed with phage-targeting crRNA plasmids, and subsequently infected with the respective viruses using spot-on-the-lawn assays (Figure 4A–C). Wild-type propagation strains (i.e. devoid of LivCRISPR-1 *cas9*/tracrRNA) and strains carrying non-targeting crRNA plasmids (pLRSR scr) served

as controls. All phages were efficiently targeted by the engineered LivCRISPR-1 system, and plaque formation was drastically reduced by at least five orders of magnitude. Control experiments demonstrated that crRNA and *cas9*/tracrRNA were required for interference, and the lack of one of these components led to complete loss of activity. We performed phage adsorption assays as an additional control to ensure that binding was not affected in any of the engineered strains (Supplementary Figure S5). It was previously shown for other type II systems that phages can escape CRISPR interference by mutation of protospacer sequences or PAMs (17). To identify the mechanism *Listeria* phages use to escape LivCRISPR-1-mediated interference, we challenged the engineered, P35- and A511-resistant strains with high multiplicities of phage and isolated a subset of naturally occurring CRISPR escape mutants (CEMs). Sequencing of the protospacer region of nineteen P35 CEMs and twenty A511 CEMs revealed frequent point mutations at nucleotide (nt) position 29 of the protospacer, and nt positions four and six of the NNACAC PAM in the CEM isolates (Figure 4D). Overall, mutations in the PAM were more frequent than in the 3′-region of the protospacer. No nucleotide changes in PAM nt position five were identified within the analyzed subset of CEMs, even though silent mutations would have been possible. This indicates that base
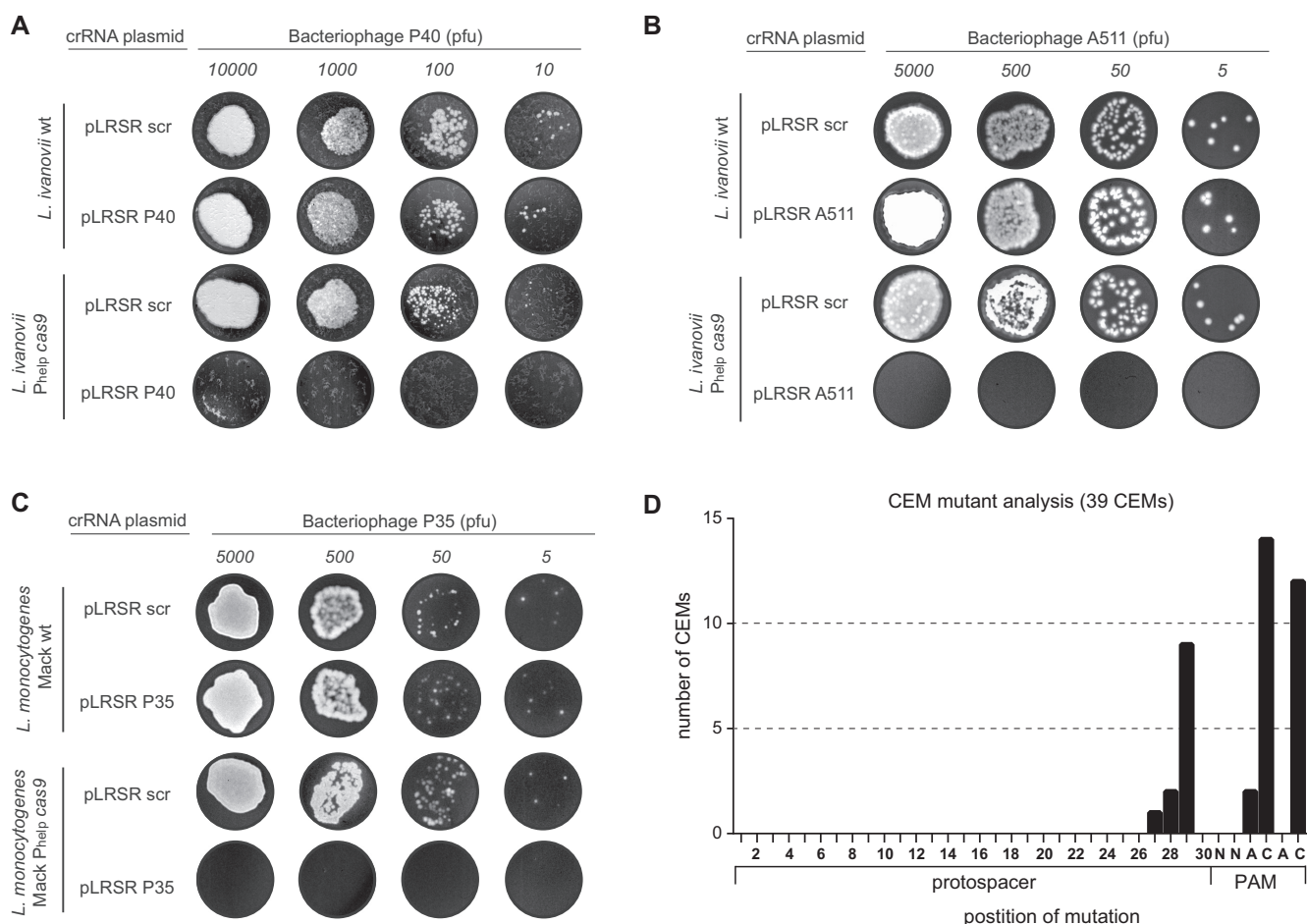
Figure 4. Using LivCRISPR-1 to construct bacteriophage insensitive mutants (BIMs). Artificial BIMs were constructed using phage propagation strains by chromosomal expression of *cas9*/tracrRNA and episomal expression of anti-phage pre-crRNA. To test for phage restriction, 5–10 000 pfu of *Listeria* phages P40 (**A**), A511 (**B**) and P35 (**C**) were spotted onto a bacterial lawn of the indicated propagation strains. Cells expressing either non-targeting crRNA and/or no *cas9*/tracrRNA served as controls. Plates were incubated for 24 h and scanned against a white background to visualize plaque formation. (**D**) To determine mutations that allow for CRISPR-escape, 19 P35 and 20 A511 CEMs were isolated from high moi infections and their protospacer and PAM regions were amplified and sequenced. Positions and frequencies of the acquired point mutations within protospacer and PAM are shown. *L. ivanovii* wt = *L. ivanovii* WSLC 3009; *L. ivanovii*::P_help *cas9* = WSLC 3009 strain expressing LivCRISPR-1 *cas9* and tracrRNA from the constitutive promoter phelp; pLRSR (scr) = pre-crRNA plasmid with non-targeting spacer; pLRSR (phage name) = pre-crRNA expression plasmid containing a spacer with 100% identity to indicated phage.

pairing at position five may not be required for interference (see Figure 4D).

LivCRISPR-1 assisted introduction of point mutations in phage A511

LivCRISPR-1 can be programmed to cleave specific bacteriophage sequences with high efficiency. This prompted us to develop a phage genome-engineering protocol based on homologous recombination of target phage DNA using a plasmid-encoded recombination template (editing plasmid, pSK1-based). In this assay, LivCRISPR-1 is used as a negative selection tool to remove wild type genomes that have not undergone recombination, thereby enriching desired recombinants (see workflow in Figure 5A). CRISPR-mediated counter-selection is required due to low recombination frequencies typically observed for on-the-fly allelic replacement during replication of phage genomes in the infected host cell (58–60). The applicability of this approach

for the introduction of single and multiple silent nucleotide substitutions into the large, 135 kilobase (kb) genome of phage A511 (48) was evaluated. For this purpose, the A511-targeting strain *L. ivanovii* 3009::P_help *cas9* pLRSR A511(see Figure 4B) was transformed with editing plasmids that contain homology arms of varying length flanking the A511 protospacer sequence (50–400 bp on each side). In addition, these editing plasmids contained one or five silent point mutations in the protospacer and PAM region (see Figure 5B). In all cases, one mutation (C→T) was introduced at nucleotide position four of the NNACAC PAM motif that allows recombinant phages to escape CRISPR interference. All strains were subsequently challenged with A511 phage using the soft-agar overlay technique and pfus were quantified (Figure 5C). A511 plating efficiency on the *cas9*-deficient control strains was approximately 10^8 pfu/ml regardless of the editing plasmid carrier state. Phage counts dropped ~10^5-fold when CRISPR-interference was active,
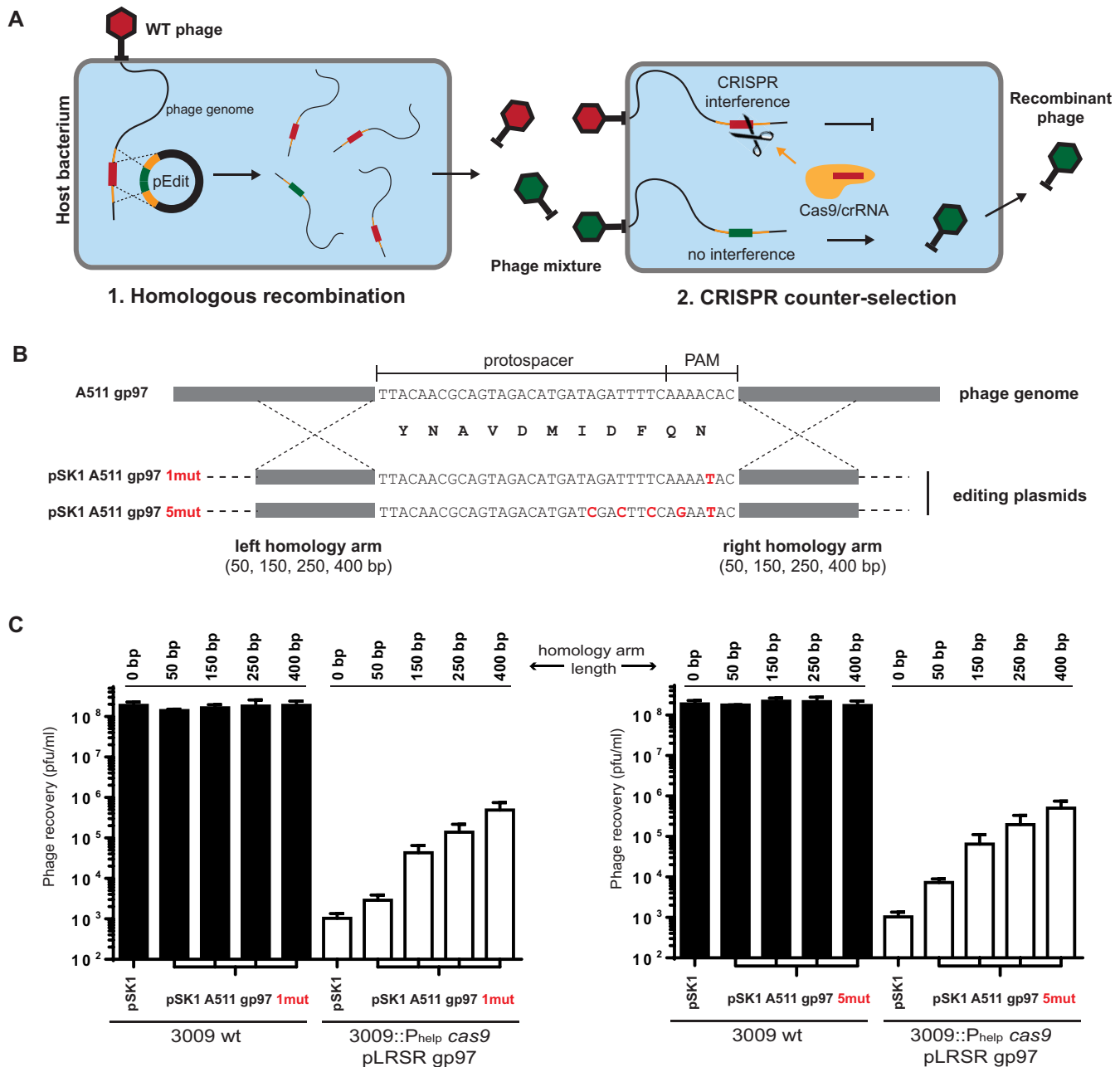
Figure 5. LivCRISPR-1-assisted site-directed mutagenesis of virulent phage genomes. (**A**) Schematic representation of the CRISPR-assisted phage genome engineering strategy. Left: The host strain carries an editing plasmid that mediates double homologous recombination with the incoming / replicating phage genome, producing a mixture of wild type and recombinant phages. Right: Engineered phages are enriched by selective, LivCRISPR-1-mediated cleavage of wild type genomes and concomitant replication of the recombinant phage. pEdit = editing plasmid. (**B**) Strategy for site-directed mutagenesis in gp97 of phage A511. Protospacer and PAM sequences in the targeted region of A511 gp97 and the corresponding editing plasmids for the incorporation of one or five silent point mutations are shown. Mutated base pairs are indicated red. Homology regions shared between the editing plasmid and the A511 gp97 gene are indicated (dashed crosses). (**C**) *L. ivanovii* WSLC 3009::Phelp *cas9* pLRSR gp97 strains were transformed with the indicated editing plasmids, infected with A511 wild type phages, and the efficiency of plating (eop) was determined. As a control, WSLC 3009 wild type strains were transformed with the same editing plasmids and eop determined. The size of the homology arms varied between 0 bp (pSK1 empty control) and 400 bp and the corresponding editing plasmids encoded either one or five silent point mutations (1mut and 5mut, respectively). Data are presented as mean ± SD from three biologically independent experiments.

and no editing template provided (pSK1 control, 0 bp). These plaques represent the background of spontaneously occurring CEMs. When providing a functional editing plasmid, phage counts increased proportionally to the length of the flanking homology arms, and reached a maximum of 6.1×10^5 and 6.2×10^5 pfu/ml for the introduction of either one or five point mutations, respectively. For each editing plasmid used in combination with CRISPR counter selection, phages recovered from single plaques were sequenced and the presence of the desired point mutations confirmed. In conclusion, we demonstrate that CRISPR-assisted genetic editing enables highly efficient introduction of multiple point mutations into virulent *Listeria* phage genomes, using a simple one-step infection protocol.

Engineering of phages for dual pathogen control

In addition to the introduction of point mutations, we tested the CRISPR engineering workflow for directed insertion of additional genes into the genome of phage A511. For this purpose, the lysostaphin gene from *Staphylococcus simulans* was selected. Lysostaphin is a metallo-endopeptidase that specifically cleaves the penta-glycine crossbridges in *Staphylococcus* peptidoglycan, and is known for its robust and selective anti-staphylococcal activity (61). We hypothesized that phage-directed production and release of lysostaphin from A511-infected *Listeria* cells would result in collateral damage, i.e. kill *S. aureus* cells present in co-culture of the two unrelated bacteria. CRISPR–Cas9 counter-selection (Figure 5A) was used to insert a hexahistidine-tagged version of lysostaphin (lysostaphin-his6) (62) either downstream of the A511 major capsid gene (yielding phage A511::*lst1*), or downstream of the A511 endolysin gene (yielding phage A511::*lst2*) (Figure 6A). Because we were unable to obtain recombinant phage in a one-step reaction, the protocol previously applied to introduce point mutations was further developed. First, A511 phage was propagated in the presence of the editing plasmid and the mixture of wild type and recombinant phage isolated. Subsequently, this phage lysate was used to infect a corresponding CRISPR interference strain for counter-selection (workflow shown in Figure 5A). Again, the editing plasmids contained single silent nucleotide substitution in one of the homology arms that allow for CRISPR escape. Using this two-step protocol, A511::*lst1* and A511::*lst2* were efficiently isolated (see Supplementary Figure S6). We show that both phage mutants infect and kill *Listeria,* but do not affect growth of *S. aureus* in single culture infection assays (Supplementary Figure S7A). Upon infection with A511::*lst1* or A511::*lst2*, we purified lysostaphin-his6 from bacterial lysates and demonstrated that both phages induce comparable levels of lysostaphin production (Supplementary Figure S7B). Next, we assessed whether the recombinant phages would be able to affect the growth of *S. aureus* in mixed cultures. *Listeria* WSLC 3009 and *S. aureus* ATCC19685 cells were co-cultured and infected with A511 wt, A511::*lst1* or A511::*lst2* at an moi of 0.03. Turbidity measurements over time demonstrated that lysostaphin-encoding phages were able to clear *Listeria*/*Staphylococcus* co-cultures within 4 h of infection (Figure 6B–C). Plating on selective media confirmed the complete eradication of both

types of bacteria at approximately 6 h post infection with either A511::*lst1* or A511::*lst2*. As expected, native A511 selectively removed only *Listeria* cells, but did not affect the growth of *S. aureus* (Figure 6D). A non-infected control culture showed similar growth of both strains in co-culture (Figure 6E). To provide visual proof, we employed fluorescently labelled cell wall-binding proteins to specifically decorate *Listeria* (GFP-CBD500) or *Staphylococcus* (dsRed-CBD2638A) cells during the experiments (28). Confocal microscopy at 0 and 5 h post infection confirmed that destruction of *Staphylococcus* cells only occurs following infection of *Listeria* cells by the engineered A511::*lst* phages (Figure 6F).

In conclusion, the LivCRISPR-1 assisted phage engineering platform represents a fast and efficient method for targeted insertion of genetic information into large, non-integrating *Listeria* phage genomes. This allows for the construction of recombinant phages with a large degree of freedom, including phages that encode additional antibacterial properties for indirect killing of bacteria by enzyme-mediated collateral damage.

DISCUSSION

Although putative CRISPR–Cas loci have been previously identified in *Listeria* (24,25), we report the first functional CRISPR–Cas interference system directly contributing to phage resistance in this organism. Interestingly, while LivCRISPR-1 *cas* gene deletion mutants became susceptible to phage B054, they remained insensitive to infection by other phages such as B025, B035 and B056, all of which bind WSLC 30167 cells (Figure 1). Recently, several new phage defense systems have been described (63–65), and some of these seem widespread in microbial genera. Doron *et al*. (63) reported several defense systems homologs in *Listeria,* predominantly in *L. monocytogenes*. However, we were unable to identify corresponding homologs in WSLC 30167, with the exception of a putative BREX system upstream of LivCRISPR-1. However, this system is incomplete, and its genetic deletion did not alter phage sensitivitiy (Supplement Figure S8, Supplementary Table S6). Collectively, this data suggests that other, yet undefined intracellular defense mechanisms await identification in this organism. It remains unclear to which extent the genus *Listeria* generally relies on CRISPR–Cas to counteract phage predation. In laboratory experiments performed under optimal growth conditions, *Listeria* BIMs isolated from high-multiplicity infection experiments most often acquire resistance by modifying cell-surface receptors. In *Listeria,* most phages bind to WTAs that provide serovar-specific glycosylation patterns (50,51). As a result of virus predation, phage-resistant WTA glycosylation mutants are rapidly selected (49). However, such alterations in cell wall structure seem to be associated with reduced environmental fitness and bacterial virulence (49–51,66). Thus, it is reasonable to assume that intracellular defense mechanisms, including CRISPR-Cas, may represent an attractive and more important defense strategy outside laboratory settings. The recent identification of anti-CRISPR proteins encoded by *Listeria* prophages (67–70) further supports this assumption.
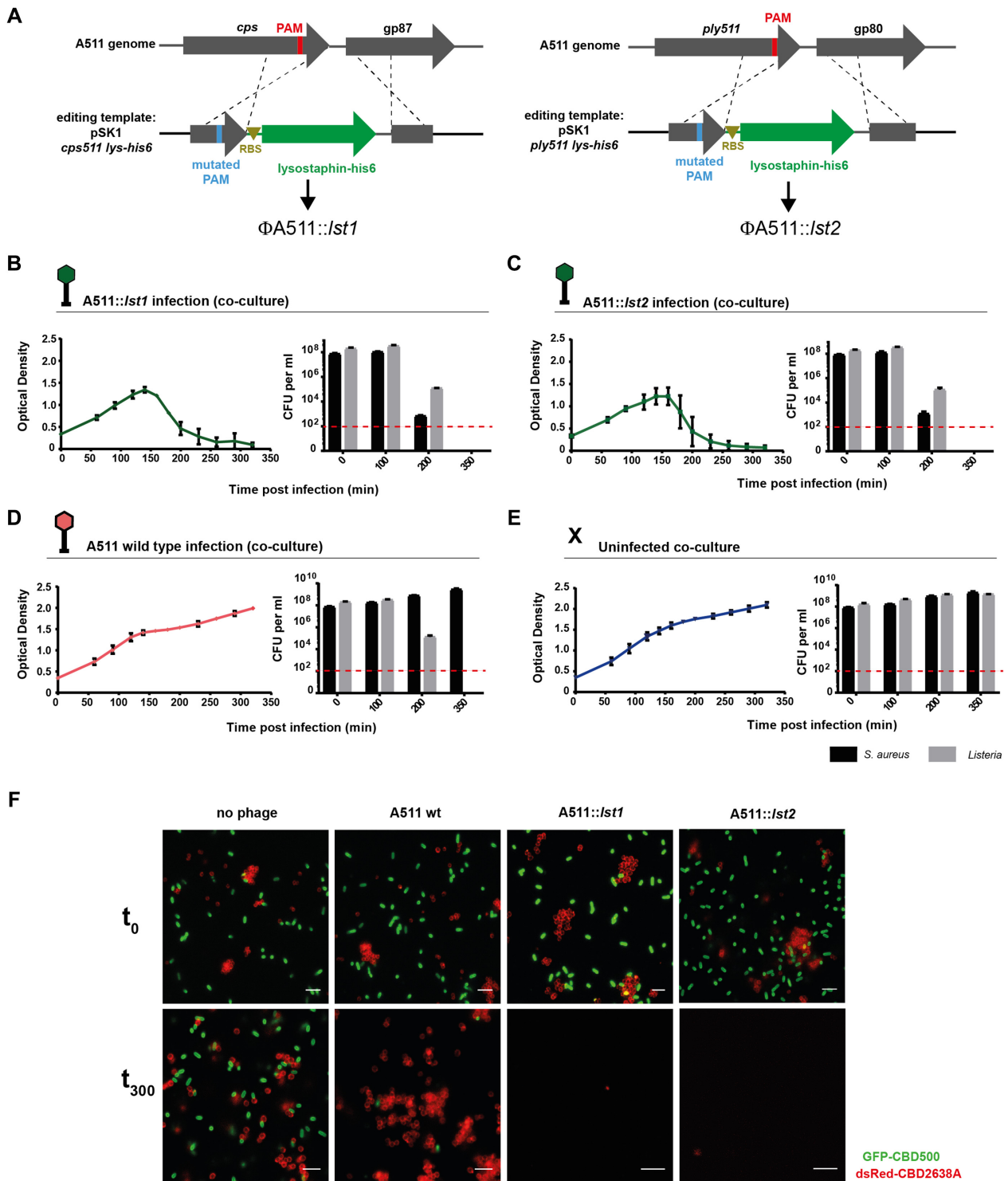
Figure 6. Lysostaphin-encoding *Listeria* phages mediate complete lysis of *Listeria* / *Staphylococcus* co-cultures. (**A**) Schematic representation of the re-combination and counter-selection strategy for the construction of lysostaphin-his6 gene insertions into A511 genomes. The protospacer and PAM regions in the wild type A511 genome that were targeted by LivCRISPR-1 are shown in red. Editing plasmids for the integration of lysostaphin downstream of the A511 major capsid gene *cps* or the A511 endolysin gene *ply511* are shown. Homologous recombination is indicated with dashed lines. Blue bars represent silent mutation in PAMs that allow recombinant phages to escape CRISPR interference. Co-cultures of *L. monocytogenes* WSLC 3009 and *S. aureus* ATCC19685 were infected with (**B**) A511::*lst1* (**C**) A511::*lst2* or (**D**) A511 wt using a non-infected culture as control (**E**). Growth of co-cultures was quantified by measuring the optical density over time (left panels) for 320 minutes and the composition of these bacterial mixtures was quantified using *Listeria*- and *Staphylococcus*-selective media (right panels). Dashed red lines indicate the detection limit of selective plating. (**F**) The composition of the infected co-cultures were visualized at time of infection (t_0) and 300 min post infection (t_{300}) using species-specific cell wall affinity proteins (GFP-CBD500 for *Listeria* and dsRed-CBD2638A for *Staphylococcus*). Data are presented as mean ± SD from three biologically independent experiments (turbidity reduction) or from a technical triplicate (selective plating). Scale bar is 4 μm.

Based on LivCRISPR-1, we developed a simple, programmable, vector-based interference system that efficiently targets and cleaves genomic DNA of *Listeria* strains and *Listeria* phages, and is active over a broad range of temperatures (Supplementary Figure S9). We also show that LivCRISPR-1 from *L. ivanovii* is active as a heterologous interference system in *L. monocytogenes* (Figure 3). Furthermore, we developed a two-step protocol for genome editing of non-integrating *Listeria* phages that combines homology-based allelic exchange with LivCRISPR-1 mediated counter-selection. To enable negative selection, the recombination template contains silent point mutations in the protospacer or PAM region that allow the recombinant phage to escape CRISPR interference. Sequence analysis of naturally occurring CEMs (Figure 4) enabled identification of the protospacer and PAM positions that are important for interference. In order for CRISPR counter-selection to work, recombination frequencies need to be higher than the frequency of naturally occurring CEMs. We provide a quantitative analysis for phage A511 and demonstrate that homology arms as short as 50–150 bps in length are sufficient to enrich recombinant phages above the background level of naturally occurring CEMs (Figure 5C).

Other than homology-directed allelic replacement, recently developed synthetic approaches also allow for rapid modification of phage genomes (71,72). To engineer phages that infect Gram-positive bacteria, virus genomes can be assembled *in-vitro* from synthetic DNA and subsequently rebooted in replicating, cell wall-deficient *Listeria* L-forms (72). However, *in-vitro* assembly of phage genomes larger than 100 kb is experimentally challenging, effectively excluding some biotechnologically relevant phage families such as the large Myoviruses, the Spounavirinae (73). This family also includes the broad host-range *Listeria* phages A511 and P100 (74). By using the CRISPR-based engineering protocol presented in this study, these highly relevant phages are now also amenable to marker-free genetic manipulation.

We applied LivCRISPR-1 to introduce additional 'payload' genes into *Listeria* phage A511. Delivery of heterologous proteins has previously been achieved in *E. coli* and *S. aureus,* using phagemids or phages (72,75–77). These applications aimed at increasing the ability of recombinant phages to kill their host strains, at re-sensitizing host bacteria to antibiotics, at creating non-replicative, antimicrobial phage particles, at targeting phage-resistant cells, or at removing antibiotic resistant bacteria (78,79). In this study, we engineered phages to deliver genes that do not directly affect the host, but instead utilize the phage as a vector and the host bacterium as a production compartment that releases a phage-encoded, heterologous effector protein upon host lysis. The effector subsequently acts on non-related bacteria that occupy the same niche, e.g. a biofilm, the gut, skin, mouth, or any other complex multispecies consortium. As proof-of-concept for this approach, we constructed *Listeria* phage A511 derivatives that carry a *Staphylococcus* cell wall-hydrolase as genetic payload and demonstrate the ability of these *Listeria* phages to kill *S. aureus* cells by collateral damage. Similar approaches could be applied to reshape more complex consortia such as misbalanced gut microbiomes that are associated with disease

(80,81). Overall, our study offers an effective and simple method for scarless genetic editing of large virulent *Listeria* phage genomes, which have previously been very difficult to engineer, also by synthetic methods.

The LivCRISPR-1 system will also be useful for RNA-guided editing of bacterial genomes. CRISPR-mediated editing of bacterial DNA has previously been achieved with Cas9 variants from *S. pyogenes* that are functional across genus barriers (e.g. in *Staphylococcus*), and even allow targeting in Gram-negative bacteria (82,83). Since LivCRISPR-1 Cas9 shows homology to Cas9 proteins from *Staphylococcus* and others (see Supplementary Figure S3), it will likely be transferrable to and active in other genera as well. Small and efficient Cas9 nucleases are highly desirable but still scarce (84). Thus, LivCRISPR-1 Cas9 may represent a particularly useful extension of the existing toolbox. It is one of the smallest active *cas9* genes known to date (3.2 kb) and requires a novel PAM sequence (NNACAC). Because the LivCRISPR-1 PAM occurs frequently (4.67 and 6.57 PAM motifs/kb in the WSLC30167 and phage A511 genomes, respectively), it is reasonable to assume that targeting of all ORFs within a typical *Firmicutes* or bacteriophage genome is feasible. CRISPR–Cas type II systems have been adapted and widely used for genome editing in eukaryotes (5,7,82,85) and it will be important to assess LivCRISPR-1 activity in eukaryotic systems in the future.

SUPPLEMENTARY DATA

Supplementary Data are available at NAR Online.

REFERENCES

1. Barrangou,R., Fremaux,C., Deveau,H., Richards,M., Boyaval,P., Moineau,S., Romero,D.A. and Horvath,P. (2007) CRISPR provides acquired resistance against viruses in prokaryotes. *Science*, **315**, 1709–1712.
2. Deveau,H., Garneau,J.E. and Moineau,S. (2010) CRISPR/Cas system and its role in phage-bacteria interactions. *Annu. Rev. Microbiol.*, **64**, 475–493.
3. Makarova,K.S., Grishin,N.V., Shabalina,S.A., Wolf,Y.I. and Koonin,E.V. (2006) A putative RNA-interference-based immune system in prokaryotes: computational analysis of the predicted enzymatic machinery, functional analogies with eukaryotic RNAi, and hypothetical mechanisms of action. *Biol. Direct*, **1**, 1.

4. Brouns,S.J., Jore,M.M., Lundgren,M., Westra,E.R., Slijkhuis,R.J., Snijders,A.P., Dickman,M.J., Makarova,K.S., Koonin,E.V. and Van Der Oost,J. (2008) Small CRISPR RNAs guide antiviral defense in prokaryotes. *Science*, **321**, 960–964.

5. Jinek,M., Chylinski,K., Fonfara,I., Hauer,M., Doudna,J.A. and Charpentier,E. (2012) A programmable dual-RNA–guided DNA endonuclease in adaptive bacterial immunity. *Science*, **337**, 816–821.

6. Deltcheva,E., Chylinski,K., Sharma,C.M., Gonzales,K., Chao,Y., Pirzada,Z.A., Eckert,M.R., Vogel,J. and Charpentier,E. (2011) CRISPR RNA maturation by trans-encoded small RNA and host factor RNase III. *Nature*, **471**, 602–607.

7. Mali,P., Yang,L., Esvelt,K.M., Aach,J., Guell,M., DiCarlo,J.E., Norville,J.E. and Church,G.M. (2013) RNA-guided human genome engineering via Cas9. *Science*, **339**, 823–826.

8. Cong,L., Ran,F.A., Cox,D., Lin,S., Barretto,R., Habib,N., Hsu,P.D., Wu,X., Jiang,W. and Marraffini,L.A. (2013) Multiplex genome engineering using CRISPR/Cas systems. *Science*, **339**, 819–823.

9. Shan,Q., Wang,Y., Li,J., Zhang,Y., Chen,K., Liang,Z., Zhang,K., Liu,J., Xi,J.J. and Qiu,J.-L. (2013) Targeted genome modification of crop plants using a CRISPR–Cas system. *Nat. Biotechnol.*, **31**, 686–688.

10. Gratz,S.J., Cummings,A.M., Nguyen,J.N., Hamm,D.C., Donohue,L.K., Harrison,M.M., Wildonger,J. and O'Connor-Giles,K.M. (2013) Genome engineering of Drosophila with the CRISPR RNA-guided Cas9 nuclease. *Genetics*, **194**, 1029–1035.

11. Barrangou,R. and van Pijkeren,J.-P. (2016) Exploiting CRISPR–Cas immune systems for genome editing in bacteria. *Curr. Opin. Biotechnol.*, **37**, 61–68.

12. Qi,L.S., Larson,M.H., Gilbert,L.A., Doudna,J.A., Weissman,J.S., Arkin,A.P. and Lim,W.A. (2013) Repurposing CRISPR as an RNA-Guided platform for Sequence-Specific control of gene expression. *Cell*, **152**, 1173–1183.

13. Bari,S.M.N., Walker,F.C., Cater,K., Aslan,B. and Hatoum-Aslan,A. (2017) Strategies for editing virulent staphylococcal phages using CRISPR–Cas10. *ACS Synth. Biol.*, **6**, 2316–2325.

14. Box,A.M., McGuffie,M.J., O'Hara,B.J. and Seed,K.D. (2016) Functional analysis of bacteriophage immunity through a Type I-E CRISPR–Cas system in vibrio cholerae and its application in bacteriophage genome engineering. *J. Bacteriol.*, **198**, 578–590.

15. Kiro,R., Shitrit,D. and Qimron,U. (2014) Efficient engineering of a bacteriophage genome using the type I-E CRISPR–Cas system. *RNA Biol.*, **11**, 42–44.

16. Lemay,M.L., Tremblay,D.M. and Moineau,S. (2017) Genome engineering of virulent lactococcal phages using CRISPR–Cas9. *ACS Synth. Biol.*, **6**, 1351–1358.

17. Martel,B. and Moineau,S. (2014) CRISPR–Cas: an efficient tool for genome engineering of virulent bacteriophages. *Nucleic Acids Res.*, **42**, 9504–9513.

18. Tao,P., Wu,X., Tang,W.C., Zhu,J. and Rao,V. (2017) Engineering of bacteriophage T4 genome using CRISPR–Cas9. *ACS Synth. Biol.*, **6**, 1952–1961.

19. Schilling,T., Dietrich,S., Hoppert,M. and Hertel,R. (2018) A CRISPR–Cas9-Based toolkit for fast and precise in vivo genetic engineering of bacillus subtilis phages. *Viruses*, **10**, E241.

20. Pires,D.P., Cleto,S., Sillankorva,S., Azeredo,J. and Lu,T.K. (2016) Genetically engineered Phages: a review of advances over the last decade. *Microbiol. Mol. Biol. Rev.*, **80**, 523–543.

21. Burstein,D., Sun,C.L., Brown,C.T., Sharon,I., Anantharaman,K., Probst,A.J., Thomas,B.C. and Banfield,J.F. (2016) Major bacterial lineages are essentially devoid of CRISPR–Cas viral defence systems. *Nat. Commun.*, **7**, 10613.

22. Makarova,K.S., Haft,D.H., Barrangou,R., Brouns,S.J.J., Charpentier,E., Horvath,P., Moineau,S., Mojica,F.J.M., Wolf,Y.I., Yakunin,A.F. *et al.* (2011) Evolution and classification of the CRISPR–Cas systems. *Nat. Rev. Microbiol*, **9**, 467–477.

23. Sorek,R., Kunin,V. and Hugenholtz,P. (2008) CRISPR––a widespread system that provides acquired resistance against phages in bacteria and archaea. *Nat. Rev. Microbiol.*, **6**, 181–186.

24. Di,H., Ye,L., Yan,H., Meng,H., Yamasak,S. and Shi,L. (2014) Comparative analysis of CRISPR loci in different *Listeria* monocytogenes lineages. *Biochem. Biophys. Res. Commun.*, **454**, 399–403.

25. Rauch,B.J., Silvis,M.R., Hultquist,J.F., Waters,C.S., McGregor,M.J., Krogan,N.J. and Bondy-Denomy,J. (2017) Inhibition of CRISPR–Cas9 with bacteriophage proteins. *Cell*, **168**, 150–158.

26. Hupfeld,M., Fouts,D.E., Loessner,M.J. and Klumpp,J. (2015) Genome sequences of the *Listeria ivanovii* subsp. ivanovii type strain and two *Listeria ivanovii* subsp. londoniensis strains. *Genome Announcements*, **3**, e01440-14.

27. Klumpp,J., Staubli,T., Schmitter,S., Hupfeld,M., Fouts,D.E. and Loessner,M.J. (2014) Genome sequences of three frequently used listeria monocytogenes and *Listeria ivanovii* strains. *Genome Announcements*, **2**, e00404-14.

28. Schmelcher,M., Shabarova,T., Eugster,M.R., Eichenseher,F., Tchang,V.S., Banz,M. and Loessner,M.J. (2010) Rapid multiplex detection and differentiation of Listeria cells by use of fluorescent phage endolysin cell wall binding domains. *Appl. Environ. Microbiol.*, **76**, 5745–5756.

29. Altschul,S.F., Gish,W., Miller,W., Myers,E.W. and Lipman,D.J. (1990) Basic local alignment search tool. *J. Mol. Biol.*, **215**, 403–410.

30. Crooks,G.E., Hon,G., Chandonia,J.-M. and Brenner,S.E. (2004) WebLogo: a sequence logo generator. *Genome Res.*, **14**, 1188–1190.

31. Söding,J., Biegert,A. and Lupas,A.N. (2005) The HHpred interactive server for protein homology detection and structure prediction. *Nucleic Acids Res.*, **33**, W244–W248.

32. Solovyev,V. and Salamov,A. (2011) Automatic annotation of microbial genomes and metagenomic sequences. *Metagenomics Applic. Agric. Biomed. Environ. Stud.*, 61–78.

33. Macke,T.J., Ecker,D.J., Gutell,R.R., Gautheret,D., Case,D.A. and Sampath,R. (2001) RNAMotif, an RNA secondary structure definition and search algorithm. *Nucleic Acids Res.*, **29**, 4724–4735.

34. Deigan,K.E., Li,T.W., Mathews,D.H. and Weeks,K.M. (2009) Accurate SHAPE-directed RNA structure determination. *Proc. Natl. Acad. Sci. U.S.A.*, **106**, 97–102.

35. Gautheret,D. and Lambert,A. (2001) Direct RNA motif definition and identification from multiple sequence alignments using secondary structure profiles1. *J. Mol. Biol.*, **313**, 1003–1011.

36. Monk,I.R., Gahan,C.G. and Hill,C. (2008) Tools for functional postgenomic analysis of Listeria monocytogenes. *Appl. Environ. Microbiol.*, **74**, 3921–3934.

37. Horton,R.M., Hunt,H.D., Ho,S.N., Pullen,J.K. and Pease,L.R. (1989) Engineering hybrid genes without the use of restriction enzymes: gene splicing by overlap extension. *Gene*, **77**, 61–68.

38. Eugster,M.R., Haug,M.C., Huwiler,S.G. and Loessner,M.J. (2011) The cell wall binding domain of Listeria bacteriophage endolysin PlyP35 recognizes terminal GlcNAc residues in cell wall teichoic acid. *Mol. Microbiol.*, **81**, 1419–1432.

39. Chakraborty,T., Leimeister-Wächter,M., Domann,E., Hartl,M., Goebel,W., Nichterlein,T. and Notermans,S. (1992) Coordinate regulation of virulence genes in Listeria monocytogenes requires the product of the prfA gene. *J. Bacteriol.*, **174**, 568–574.

40. Beasley,S., Takala,T., Reunanen,J., Apajalahti,J. and Saris,P. (2004) Characterization and electrotransformation of Lactobacillus crispatus isolated from chicken crop and intestine. *Poultry Sci.*, **83**, 45–48.

41. Goldberg,G.W., Jiang,W., Bikard,D. and Marraffini,L.A. (2014) Conditional tolerance of temperate phages via transcription-dependent CRISPR–Cas targeting. *Nature*, **514**, 633–637.

42. Lauer,P., Chow,M.Y.N., Loessner,M.J., Portnoy,D.A. and Calendar,R. (2002) Construction, characterization, and use of two listeria monocytogenes Site-Specific phage integration vectors. *J. Bacteriol.*, **184**, 4177–4186.

43. Liu,D. (2008) *Handbook of Listeria monocytogenes*. CRC Press.

44. Seeliger,H. and Hönne,K. Serotyping of Listeria monocytogenes and related species. Vol. 13. *Methods Microbiol. Capítulo*, **11**, 31–49.

45. Shen,Y., Boulos,S., Sumrall,E., Gerber,B., Julian-Rodero,A., Eugster,M.R., Fieseler,L., Nystrom,L., Ebert,M.O. and Loessner,M.J. (2017) Structural and functional diversity in Listeria cell wall teichoic acids. *J. Biol. Chem.*, **292**, 17832–17844.

46. Boerlin,P., Rocourt,J., Grimont,F., Grimont,P.A.D., Jacquet,C. and Piffaretti,J.-C. (1992) *Listeria ivanovii* subsp. londoniensis subsp. nov. *Int. J. Syst. Bacteriol.*, **42**, 69–73.

47. Klumpp,J. and Loessner,M.J. (2013) *Listeria* phages: genomes, evolution, and application. *Bacteriophage*, **3**, e26861.

48. Klumpp,J., Dorscht,J., Lurz,R., Bielmann,R., Wieland,M., Zimmer,M., Calendar,R. and Loessner,M.J. (2008) The terminally redundant, nonpermuted genome of listeria bacteriophage A511: a model for the SPO1-Like myoviruses of Gram-positive bacteria. *J. Bacteriol.*, **190**, 5753–5765.

49. Eugster,M.R., Morax,L.S., Hüls,V.J., Huwiler,S.G., Leclercq,A., Lecuit,M. and Loessner,M.J. (2015) Bacteriophage predation promotes serovar diversification in Listeria monocytogenes. *Mol. Microbiol.*, **97**, 33–46.

50. Habann,M., Leiman,P.G., Vandersteegen,K., Van den Bossche,A., Lavigne,R., Shneider,M.M., Bielmann,R., Eugster,M.R., Loessner,M.J. and Klumpp,J. (2014) Listeria phage A511, a model for the contractile tail machineries of SPO1-related bacteriophages. *Mol. Microbiol.*, **92**, 84–99.

51. Bielmann,R., Habann,M., Eugster,M.R., Lurz,R., Calendar,R., Klumpp,J. and Loessner,M.J. (2015) Receptor binding proteins of Listeria monocytogenes bacteriophages A118 and P35 recognize serovar-specific teichoic acids. *Virology*, **477**, 110–118.

52. Chylinski,K., Makarova,K.S., Charpentier,E. and Koonin,E.V. (2014) Classification and evolution of type II CRISPR–Cas systems. *Nucleic Acids Res.*, **42**, 6091–6105.

53. Friedland,A.E., Baral,R., Singhal,P., Loveluck,K., Shen,S., Sanchez,M., Marco,E., Gotta,G.M., Maeder,M.L., Kennedy,E.M. *et al.* (2015) Characterization of Staphylococcus aureus Cas9: a smaller Cas9 for all-in-one adeno-associated virus delivery and paired nickase applications. *Genome Biol.*, **16**, 257.

54. Ran,F.A., Cong,L., Yan,W.X., Scott,D.A., Gootenberg,J.S., Kriz,A.J., Zetsche,B., Shalem,O., Wu,X., Makarova,K.S. *et al.* (2015) In vivo genome editing using Staphylococcus aureus Cas9. *Nature*, **520**, 186–191.

55. Karvelis,T., Gasiunas,G. and Siksnys,V. (2017) Methods for decoding Cas9 protospacer adjacent motif (PAM) sequences: a brief overview. *Methods*, **121–122**, 3–8.

56. Sorek,R., Lawrence,C.M. and Wiedenheft,B. (2013) CRISPR-mediated adaptive immune systems in bacteria and archaea. *Annu. Rev. Biochem.*, **82**, 237–266.

57. Dorscht,J., Klumpp,J., Bielmann,R., Schmelcher,M., Born,Y., Zimmer,M., Calendar,R. and Loessner,M.J. (2009) Comparative genome analysis of Listeria bacteriophages reveals extensive mosaicism, programmed translational frameshifting, and a novel prophage insertion site. *J. Bacteriol.*, **191**, 7206–7215.

58. Loessner,M.J., Rees,C., Stewart,G. and Scherer,S. (1996) Construction of luciferase reporter bacteriophage A511:: luxAB for rapid and sensitive detection of viable Listeria cells. *Appl. Environ. Microbiol.*, **62**, 1133–1140.

59. Le,S., He,X., Tan,Y., Huang,G., Zhang,L., Lux,R., Shi,W. and Hu,F. (2013) Mapping the tail fiber as the receptor binding protein responsible for differential host specificity of Pseudomonas aeruginosa bacteriophages PaP1 and JG004. *PLoS One*, **8**, e68562.

60. Mahichi,F., Synnott,A.J., Yamamichi,K., Osada,T. and Tanji,Y. (2009) Site-specific recombination of T2 phage using IP008 long tail fiber genes provides a targeted method for expanding host range while retaining lytic activity. *FEMS Microbiol. Lett.*, **295**, 211–217.

61. Bastos,M., Ceotto,H., Coelho,M. and Nascimento,J. (2009) Staphylococcal antimicrobial peptides: relevant properties and potential biotechnological applications. *Curr. Pharmaceut. Biotechnol.*, **10**, 38–61.

62. Schmelcher,M., Shen,Y., Nelson,D.C., Eugster,M.R., Eichenseher,F., Hanke,D.C., Loessner,M.J., Dong,S., Pritchard,D.G. and Lee,J.C. (2015) Evolutionarily distinct bacteriophage endolysins featuring conserved peptidoglycan cleavage sites protect mice from MRSA infection. *J. Antimicrob. Chemother.*, **70**, 1453–1465.

63. Doron,S., Melamed,S., Ofir,G., Leavitt,A., Lopatina,A., Keren,M., Amitai,G. and Sorek,R. (2018) Systematic discovery of antiphage defense systems in the microbial pangenome. *Science*, **359**, eaar4120.

64. Goldfarb,T., Sberro,H., Weinstock,E., Cohen,O., Doron,S., Charpak-Amikam,Y., Afik,S., Ofir,G. and Sorek,R. (2015) BREX is a novel phage resistance system widespread in microbial genomes. *EMBO J.*, **34**, 169–183.

65. Ofir,G., Melamed,S., Sberro,H., Mukamel,Z., Silverman,S., Yaakov,G., Doron,S. and Sorek,R. (2018) DISARM is a widespread bacterial defence system with broad anti-phage activities. *Nat. Microbiol.*, **3**, 90–98.

66. Wendlinger,G., Loessner,M.J. and Scherer,S. (1996) Bacteriophage receptors on Listeria monocytogenes cells are the N-acetylglucosamine and rhamnose substituents of teichoic acids or the peptidoglycan itself. *Microbiology*, **142**, 985–992.

67. Rauch,B.J., Silvis,M.R., Hultquist,J.F., Waters,C.S., McGregor,M.J., Krogan,N.J. and Bondy-Denomy,J. (2017) Inhibition of CRISPR–Cas9 with bacteriophage proteins. *Cell*, **168**, 150–158.

68. Dong,D., Guo,M., Wang,S., Zhu,Y., Wang,S., Xiong,Z., Yang,J., Xu,Z. and Huang,Z. (2017) Structural basis of CRISPR–SpyCas9 inhibition by an anti-CRISPR protein. *Nature*, **546**, 436–439.

69. Yang,H. and Patel,D.J. (2017) Inhibition mechanism of an Anti-CRISPR suppressor AcrIIA4 targeting SpyCas9. *Mol. Cell*, **67**, 117–127.

70. Pawluk,A., Davidson,A.R. and Maxwell,K.L. (2018) Anti-CRISPR: Discovery, mechanism and function. *Nat. Rev. Microbiol.*, **16**, 12.

71. Ando,H., Lemire,S., Pires,D.P. and Lu,T.K. (2015) Engineering modular viral scaffolds for targeted bacterial population editing. *Cell Syst.*, **1**, 187–196.

72. Kilcher,S., Studer,P., Muessner,C., Klumpp,J. and Loessner,M.J. (2018) Cross-genus rebooting of custom-made, synthetic bacteriophage genomes in L-form bacteria. *Proc. Natl. Acad. Sci. U.S.A.*, **115**, 567–572.

73. Klumpp,J., Lavigne,R., Loessner,M. and Ackermann,H.-W. (2010) The SPO1-related bacteriophages. *Archiv. Virol.*, **155**, 1547–1561.

74. Carlton,R.M., Noordman,W.H., Biswas,B., de Meester,E.D. and Loessner,M.J. (2005) Bacteriophage P100 for control of Listeria monocytogenes in foods: genome sequence, bioinformatic analyses, oral toxicity study, and application. *Regul. Toxicol. Pharmacol.*, **43**, 301–312.

75. Lu,T.K. and Collins,J.J. (2007) Dispersing biofilms with engineered enzymatic bacteriophage. *Proc. Natl. Acad. Sci. U.S.A.*, **104**, 11197–11202.

76. Lu,T.K. and Collins,J.J. (2009) Engineered bacteriophage targeting gene networks as adjuvants for antibiotic therapy. *Proc. Natl. Acad. Sci. U.S.A.*, **106**, 4629–4634.

77. Westwater,C., Kasman,L.M., Schofield,D.A., Werner,P.A., Dolan,J.W., Schmidt,M.G. and Norris,J.S. (2003) Use of genetically engineered phage to deliver antimicrobial agents to bacteria: an alternative therapy for treatment of bacterial infections. *Antimicrob. Agents Chemother.*, **47**, 1301–1307.

78. Bikard,D., Euler,C.W., Jiang,W., Nussenzweig,P.M., Goldberg,G.W., Duportet,X., Fischetti,V.A. and Marraffini,L.A. (2014) Exploiting CRISPR–Cas nucleases to produce sequence-specific antimicrobials. *Nat. Biotechnol.*, **32**, 1146–1150.

79. Citorik,R.J., Mimee,M. and Lu,T.K. (2014) Sequence-specific antimicrobials using efficiently delivered RNA-guided nucleases. *Nat. Biotechnol.*, **32**, 1141–1145.

80. Cho,I. and Blaser,M.J. (2012) The human microbiome: at the interface of health and disease. *Nat. Rev. Genet.*, **13**, 260.

81. Zmora,N., Zeevi,D., Korem,T., Segal,E. and Elinav,E. (2016) Taking it personally: personalized utilization of the human microbiome in health and disease. *Cell Host Microbe*, **19**, 12–20.

82. Jiang,W., Bikard,D., Cox,D., Zhang,F. and Marraffini,L.A. (2013) RNA-guided editing of bacterial genomes using CRISPR–Cas systems. *Nat. Biotechnol.*, **31**, 233–239.

83. Chen,W., Zhang,Y., Yeo,W.-S., Bae,T. and Ji,Q. (2017) Rapid and efficient genome editing in staphylococcus aureus by using an engineered CRISPR/Cas9 system. *J. Am. Chem. Soc.*, **139**, 3790–3795.

84. Ran,F.A., Cong,L., Yan,W.X., Scott,D.A., Gootenberg,J.S., Kriz,A.J., Zetsche,B., Shalem,O., Wu,X. and Makarova,K.S. (2015) In vivo genome editing using Staphylococcus aureus Cas9. *Nature*, **520**, 186.

85. Xu,K., Ren,C., Liu,Z., Zhang,T., Zhang,T., Li,D., Wang,L., Yan,Q., Guo,L. and Shen,J. (2015) Efficient genome engineering in eukaryotes using Cas9 from Streptococcus thermophilus. *Cell. Mol. Life Sci.*, **72**, 383–399.